1 **Title: Juvenile corals underpin coral reef carbonate production after disturbance**

2

3 **Authors:** Jérémy Carlot[1,2]*, Mohsen Kayal[3], Hunter S. Lenihan[4], Simon J. Brandl[1,2,5,6], Jordan

4 M. Casey[1,2,6], Mehdi Adjeroud[1,2,7], Ulisse Cardini[8,9], Alexandre Merciere[10], Benoit Espiau[10],

5 Diego R. Barneche[11], Alessio Rovere[12], Laetitia Hédouin[10,2], Valeriano Parravicini[1,2]

6

7 Jérémy Carlot 0000-0003-0887-8005

8 Mohsen Kayal 0000-0003-3675-9855

9 Hunter S. Lenihan 0000-0001-8146-7670

10 Simon J. Brandl 0000-0002-6649-2496

11 Jordan M. Casey 0000-0002-2434-7207

12 Mehdi Adjeroud 0000-0002-6825-8759

13 Ulisse Cardini 0000-0002-0816-6158

14 Diego R. Barneche 0000-0002-4568-2362

15 Alessio Rovere 0000-0001-5575-1168

16 Valeriano Parravicini 0000-0002-3408-1625

17

18 **Affiliations:**

[1]PSL Université Paris, USR 3278 CRIOBE - EPHE-UPVD-CNRS, Perpignan, France

[2]Laboratoire d'Excellence "CORAIL", Paris, France

[3]ENTROPIE, IRD, Université de la Réunion, CNRS, IFREMER, Université de la Nouvelle-Calédonie, Nouméa, New-Caledonia

[4]Bren School of Environmental Science and Management, University of California, Santa Barbara, CA USA 93106

[5]CESAB - FRB, 5 Rue de l'École de Médecine, 34000, Montpellier

[6]Department of Marine Science, University of Texas at Austin, Marine Science Institute, Port Aransas, Texas, USA

[7]ENTROPIE, IRD, Université de la Réunion, CNRS, Perpignan, France

[8]Integrative Marine Ecology Department, Stazione Zoologica Anton Dohrn, National Institute of Marine Biology, Ecology and Biotechnology, Napoli, Italy

[9]Marine Research Institute, University of Klaipeda, Klaipeda, Lithuania

[10]PSL Université - EPHE-UPVD-CNRS, USR 3278 CRIOBE, Papetoai, French Polynesia

[11]Australian Institute of Marine Science, Crawley, WA 6009, Australia

[12]Centre for Marine Environmental Sciences (MARUM), Bremen, Germany

* Corresponding author. Email: jay.crlt02@gmail.com

Abstract: Sea-level rise is predicted to cause major damage to tropical coastlines. While coral reefs can act as natural barriers for ocean waves, their protection hinges

on the ability of scleractinian corals to produce enough calcium carbonate ($CaCO_3$) to keep up with rising sea levels. As a consequence of intensifying disturbances, coral communities are changing rapidly, potentially reducing community-level $CaCO_3$ production. By combining colony-level physiology and long-term monitoring data, we show that reefs recovering from major disturbances can produce 40% more $CaCO_3$ than currently estimated due to the disproportionate contribution of juvenile corals. However, the buffering effect of highly productive juvenile corals is compromised by recruitment failures, which have been more frequently observed after large-scale, repeated bleaching events. While the size structure of corals can bolster a critical ecological function on reefs, climate change impacts on recruitment may undermine this buffering effect, thus further compromising the persistence of reefs and their provision of important ecosystem services.

Abstract: coral juveniles – $CaCO_3$ production – reef productivity – coral assemblages – time series – calcification rates – linear extension

One Sentence Summary: Juvenile corals underpin reef recovery in a changing world

1 | INTRODUCTION

The Intergovernmental Panel on Climate Change (IPCC) predicts a climate-driven sea-level rise of 0.43m to 0.84m by 2100 (Oppenheimer et al., 2019), thus increasing the risk of coastal flooding, especially during tropical storms (Ellison et al., 2019; Nunn et al., 2017; Tebaldi et al., 2012). Sea-level rise will be amplified in the tropics, where vulnerable ecosystems such as mangroves and coral reefs act as natural barriers to protect more than 500 million people from oceanic waves (Hoegh-Guldberg et al., 2007). For coasts protected by coral reefs, their future exposure to oceanic waves will largely depend on the ability of scleractinian corals to produce enough calcium carbonate ($CaCO_3$) for reefs to grow vertically at a rate equivalent to sea-level rise. However, reefs are increasingly threatened by both climate change and local anthropogenic disturbances (Darling et al., 2019; Hughes et al., 2017). Climate-induced coral bleaching is expected to become an annual phenomenon for most coral reefs within the next twenty years (van Hooidonk et al., 2016), inducing a state of constant disturbance that decreases the likelihood of recovery. Whether reefs anmd their services will persist is presently unknown and requires the assessment of reef

$CaCO_3$ production across disturbance-recovery cycles (Harris et al., 2018; Perry, Alvarez-Filip, et al., 2018).

The quantification of $CaCO_3$ production (kg m^{-2} yr^{-1}) for reefscapes is traditionally based on species-specific linear extension rates of corals combined with the proportional substratum cover of the species. In most cases, this is applied to each colony regardless of their size (Perry, Lange, et al., 2018). Depending on the coral growth form, this scaling process relies on the assumption that species-specific $CaCO_3$ production rates are constant throughout coral ontogeny. However, this may not always be the case as $CaCO_3$ production rates may be either allometric or isometric (Fig. 1). In the case of isometry, $CaCO_3$ production rate scales linearly with colony size; conversely, in the case of allometry, $CaCO_3$ production rate either accelerates or decelerates as colonies grow. While it is often assumed that the coral colony-level production of $CaCO_3$ is isometric, recent work suggests that coral growth (expressed as an increase in planar area) is allometric, either because large colonies experience higher rates of partial-mortality (Madin et al., 2020) and/or because coral colonies allocate less energy to $CaCO_3$ production in favor of reproduction once they reach a certain size (Kayal et al., 2015). Whether coral growth is indeed isometric or allometric

remains poorly resolved, but may significantly influence our community-wide estimates of $CaCO_3$ production (Fig. 1). If corals grow allometrically, assuming isometry may lead to an underestimation of the production by small colonies and significantly obscure overarching estimates of $CaCO_3$ production patterns across reefscapes.

Recent climate-driven disturbances, especially catastrophic coral-bleaching events and major storms, can substantially alter the size-distribution of coral assemblages (Dietzel et al., 2020). Large perturbations often remove a substantial proportion of large coral colonies and leave the remaining assemblage dominated by small corals (Alvarado et al., 2016; Holbrook et al., 2018). In these situations, isometric approaches may lead to a severe underestimation of overall $CaCO_3$ production, thus inhibiting our ability to infer a reef's ability to regain coral cover. Yet, the loss of large corals may also significantly reduce overall fecundity, leading to reduced coral recruitment and thus inhibiting coral recovery (Hughes & Tanner, 2000). This negative feedback loop can diminish the overall productivity of reefs over time (Hughes et al., 2019). According to recent estimates, most coral reefs have a net production of $CaCO_3$ close to zero (Perry, Alvarez-Filip, et al., 2018; Woodroffe & Webster, 2014).

Therefore, even slight differences in $CaCO_3$ production may have major implications for the capacity of reefs to survive despite sea-level rise.

Here we estimate **$CaCO_3$ production** rates of three prominent coral genera over a range of colony sizes and test whether $CaCO_3$ production follows an allometric or isometric growth pattern. We then use an empirical time-series dataset from French Polynesia that reports the size of individual coral colonies across a ten-year disturbance-recovery cycle to examine whether the conventional isometric approach leads to an incorrect estimation of community-level $CaCO_3$ production. Finally, we evaluate the outcome of large-scale disturbances, such as a major bleaching event, simulating the effect of recruitment loss on $CaCO_3$ production over five years.

2 | METHODS

2 .1 | $CaCO_3$ production using *in situ* alizarin red-S staining

In June 2018, we used the approach described by Dustan (1975) to stain 175 coral colonies of ***Acropora hyacinthus*** (n = 50), ***Pocillopora verrucosa*** (n = 75), and ***Porites lutea*** (n = 50) ***in situ*** at a depth of 10 to 15 m on the outer reef slopes

around the island of Mo'orea (French Polynesia, Fig. S1). Before staining, we measured the length, width, and height of each coral colony. **We stained colonies with a surface area ranging from 140 cm^2 (i.e. ~5 cm diameter) to 3,850 cm^2 (i.e. ~80 cm diameter), which broadly matches the range of coral colony sizes observed in Mo'orea (Kayal et al., 2018 ; coral colonies observed *in situ* ranged from <1 cm^2 to ~5000 cm^2).** We enclosed each coral in a 5, 10, or 20 L transparent plastic bag, filled with 10 mg L^{-1} of alizarin red-S, for 72 hours. All colonies were tagged and mapped for future retrieval. To minimize the confounding effects of competition on growth, we chose colonies that were not in direct contact with other corals. **In December 2018, 74% of colonies (n = 130) were recovered** and three fragments were collected from each coral for growth measurements. **We reasoned that a 6 month period was representative of the mean annual growth rate, since it covered the average temperatures typical for the cooler (26°C) and warmer (29°C) seasons in Mo'orea (*cf.* Smith et al., 2007).** Samples were dried for 48 hours and placed into transparent epoxy for 24 hours before slicing three 0.7 mm thick slices from each colony using a diamond-tipped saw, perpendicular to the major axis of growth. **We took high-resolution photos of each colony slice using fluorescence, and calculated linear extension as the average of three measurements**

(i.e., length, width, and height) per colony (Fig. S2). We also measured the longest linear extension from the edge of the stain to the periphery of the skeleton to the nearest 0.1mm using Image J software (Schneider et al., 2012). Finally, we calculated the $CaCO_3$ production rate using the equation C = (LE × D) × AC, where C represents the $CaCO_3$ production rate (g cm^{-2} yr^{-1}), LE represents the linear extension (cm yr^{-1}), D represents the skeletal density, measured by the buoyed weight displacement method (respectively 1.4, 1.5 and 1.3 g cm^{-3} for *A. hyacinthus, P. verrucosa* and *P. lutea*), and AC represents the adjustment coefficient (between 0 and 1), depending on the growth form of the colony (Morgan and Kench 2012). We used an AC of 0.4, 0.5, and 1 for *A. hyacinthus, P. verrucosa,* and *P. lutea,* respectively.

2 .2 | $CaCO_3$ production using alkalinity anomaly *ex situ* incubations

To characterize $CaCO_3$ production in smaller colonies, for which the Alizarin red-S approach was not feasible, we removed 96 coral colonies [*A. hyacinthus* (n = 25), *P. verrucosa* (n = 25) and *P. lutea* (n = 46)] with surface areas of 35–1,000 cm^2 (*i.e.,* ~3–15 cm diameter) from the north shore of Mo'orea (depth = 12m) using a hammer and chisel. Before each collection, we recorded relevant environmental

157 parameters (mean ambient seawater temperature, salinity, and photosynthetically
158 active radiation). Upon return to the surface, we placed colonies in seawater tanks
159 under the same environmental conditions for recovery and acclimation. Sponges,
160 crustose coralline algae (CCA), macro-algae, epiphytes, and small crustaceans were
161 carefully removed from the corals. We measured the length, width, and height of each
162 colony, then tagged and kept the corals in the acclimation tank for 7 days. 73% of the
163 colonies (n = 70) did not show any obvious adverse reactions to collected and handled,
164 so we retained them for $CaCO_3$ production measurements. **Coral colonies were**
165 **grouped into three different size classes (<100 cm^2, 100–400 cm^2, and 400–1000**
166 **cm^2—see section 2.3). Size selection for the incubation chambers was based on**
167 **providing sufficient water volume for each coral colony, while ensuring traceability of**
168 **changes in water chemistry (Kolb, 2018). Consequently, colonies were incubated in**
169 **chambers of three different volumes (0.5, 1, and 4 L, respectively) to maintain a**
170 **relatively constant incubation volume to colony size ratio.** Four additional incubation
171 chambers were used as blank controls. Each week, we assessed four controls and
172 four corals of each size class. Water samples of 50 mL were collected from the
173 incubation controls and each chamber after three hours of incubation for total alkalinity

analysis. We made sure that coral colonies did not experience O_2 reductions of more than 80% (Kolb, 2018), in which case observations were removed from the dataset. We defined net $CaCO_3$ production by assuming a mole of $CaCO_3$ is produced when the alkalinity measure (ΔAT) drops by two moles for a fixed time (Δt) (S. V Smith & Key, 1975). By multiplying these parameters ($-\Delta AT/2.\Delta t$) by seawater density (ρ_{sw}), we defined the global $CaCO_3$ production rate, which was then normalized with live coral surface area and converted to g cm^{-2} yr^{-1} based on the molar $CaCO_3$ mass (Dickson et al., 2007).

2 .3 | Photogrammetry-based size area relationships

To examine the relationship between $CaCO_3$ production and colony size, we used a 3D surface area to avoid underestimating coral $CaCO_3$ production, as surface folding and branching increase the coral surface area. Following the coral incubation protocol, 100 to 200 overlapping high-resolution photos were taken for each colony **(Fig. S3)**. The photos were used to construct 3D **models** using Agisoft PhotoScan (LLC Agisoft Photosocan, 2016). We defined volume and live surface area from the final 3D model (i.e., outside area of the coral minus the base). We fitted a power-law regression

191 between coral colony mean diameter (i.e., mean of the 3 dimensions defined for each
192 colony) and coral live surface area (R^2 = 0.97) (Kayal et al., 2015). This relationship
193 was used to estimate the surface area of the coral colonies measured during the
194 alizarin red-S staining, incubation experiments, and size distribution surveys.
195
196 **2 .4 | Bayesian $CaCO_3$ production models**
197 To test whether $CaCO_3$ production of the three coral genera followed an
198 allometric or isometric pattern, we first verified that the $CaCO_3$ production from *in situ*
199 alizarin red-S staining and *ex situ* incubations were analogous. Alizarin red-S staining
200 has the advantage of providing data from corals *in situ* (i.e., growing under normal
201 environmental conditions). However, given the potential for toxicity in juvenile corals
202 (Dustan, 1975), $CaCO_3$ production of juveniles is better estimated with *ex situ*
203 incubations. In our study, alizarin red-S staining and alkalinity anomaly incubation
204 yielded similar results **for $CaCO_3$ production (Fig. S4)**; therefore, we merged the
205 datasets to estimate isometric and allometric relationships with Bayesian inference as
206 follows:
207

$$C_i \sim N(\mu_i, \sigma^2), \text{ Allometric model: } \mu_i = \alpha x_i^{\beta}$$

$$\text{Isometric model: } \mu_i = \alpha x_i + \beta$$

where C_i is the $CaCO_3$ production rate (g yr^{-1}) and x_i the live coral surface area (cm^2). We specified the same priors for both models (α ~ Normal (10,10) and β ~ Normal (0.5,0.5)) with a weakly-informative variance (σ^2 ~ Student (3,0,450)). We fitted our models with 3000 iterations across four chains, and discarded the first 1500 warm-up iterations of each chain. We verified chain convergence with visual inspection and confirmed that Rhat (the potential scale-reduction factor) was less than 1.05. Using the model summary parameters, we then predicted both $CaCO_3$ production and area-normalized $CaCO_3$ production rates (± 95% Bayesian credible interval).

2 .5 | Coral community $CaCO_3$ production

We used both isometric and allometric functions for quantifying community wide $CaCO_3$ production to test whether the two approaches yielded different results when coral size distribution changes over time. Between 2005 and 2016, Mo'orea experienced an outbreak of the predatory sea star *Acanthaster* cf. *solaris* (2006-2009),

followed by a cyclone (2010). The two disturbances reduced live coral cover from approximately 50% in 2005 to 3% in 2010 (Carlot et al., 2020; Kayal et al., 2012). Following the disturbances, coral cover recovered to pre-disturbance levels by 2016 (Kayal et al., 2018 ; Fig. 2). The change in coral cover was accompanied by considerable variations in coral size distributions. Large colonies were dominant in 2005 (Table S1) but were dramatically outnumbered by small recruits in 2011 (Adjeroud et al., 2018). We applied both $CaCO_3$ production models (i.e., isometric *versus* allometric) at the community level by combining data from three studies that recorded temporal changes in size distributions of the three major reef-building corals around Mo'orea. The first study evaluated coral size distributions in 2005 (Adjeroud et al., 2015), the second study took place from 2008-2010 (Kayal et al., 2015) and the third study was conducted from 2011-2016 (Kayal et al., 2018) as part of the Mo'orea Coral Reef Long Term Ecological Research program (LTER; http://mcr.lternet.edu). All surveys were conducted at a minimum of three different sites around Mo'orea at a depth of approximatively 12m.

Due to heterogeneity among datasets (i.e., differences in survey protocols, efforts, sites and observers), we standardized the data by pooling all transects for a

given year to obtain an island-scale coral size distribution for each taxon, from which we estimated population abundances matching the percent cover of the species at each site. To do so, we assumed that the planar shape of our three species is approximated by a circle when observed from above. We then calculated individual colony planar areas from visually-determined length and width (i.e., ((length + width)/4)$^2\pi$). In some of the studies, coral size distribution was evaluated without recording the sampling effort (e.g., by recording the size of the 50 first colonies intercepted along a transect). Therefore, we evaluated coral density per 10m^2 substrate by randomly sampling individuals from our island-scale size distribution dataset until matching the percent cover of the species in each year. We repeated this process 100 times to obtain an average island-scale coral size distribution per taxa per year. We compared our coral size-distributions estimates with empirical data collected in 2009 by Kayal et al. (2015) for the three coral species and found no significant difference (Fig. S4). Annual changes in coral cover for the three coral genera were estimated as part of the "*Service d'Observatoire CORAIL*" monitoring (SO CORAIL monitoring; http://observatoire.criobe.pf). We then assigned $CaCO_3$ production to each colony and summed them to yield total production per 10m^2 of reef.

259

260 **2 .6 | Recruitment loss model**

261 To estimate how large-scale disturbance events may impact reef $CaCO_3$

262 production, we used a multi-species, open-population, integral projection model (IPM)

263 developed to characterize coral community dynamics around Mo'orea (Kayal et al.,

264 2018). The IPM predicted recovery dynamics in the abundance, composition, and size

265 distribution of coral assemblages (i.e., *Acropora*, *Pocillopora,* and *Porites*) after the

266 2006-2010 disturbances (Fig. S6). For each population, the model is governed by the

267 following:

268

269 $$n\,(z',t+1)=\int_{Low}^{Up} s\,(z)\mathrm{G}\,(z,z')\mathrm{n}\,(z,\mathrm{t})\mathrm{d}z + R\,(\gamma,z')$$

270

271 where the distribution of individuals n (z', t+1) of final-size z' at time t+1 is predicted as

272 a function of the distribution of the individuals n (z, t) of sizes z, bounded to the size-

273 range interval [*Low*, *Up*], at time t. The functions s, G, and R describe empirically

274 estimated size (z) dependent survival and growth, and density (γ) dependent

275 recruitment, respectively.

We used the IPM to simulate the recovery of coral assemblages from 2010 to 2015 according to different recruitment scenarios. Specifically, we compared reef recovery under the observed recruitment rates (present-day scenario R×1) *versus* different scenarios of decline where recruitment was restricted to 75%, 50%, and 25% of the observed values (scenarios R×0.75, R×0.5, and R×0.25, respectively). The model was implemented with estimates of coral demographic parameters based on empirically measured coral survival, growth, and recruitment rates on the north shore of Mo'orea, where coral recruitment and recovery achieved maximum levels in 2010-2015 (Kayal et al., 2018). Finally, the allometric Bayesian model was applied to the distribution of the coral colonies' surface area predicted under the four recruitment scenarios (Fig. S6) to estimate $CaCO_3$ production rates (Fig. 4). All statistics and predictive models were run using the *brms* and *nlme* packages (Bürkner, 2017b, 2017a; Pinheiro et al., 2013) in R version 3.5.3 (R Core Team, 2019).

3 | RESULTS

All three coral species exhibited an allometric linear extension pattern, with small coral colonies producing disproportionately larger amounts of $CaCO_3$ per unit

surface area than larger colonies (Fig. 3). For example, a fivefold increase in colony surface area from 100 to 500 cm^2 led to a 26% decline in linear extension for *Acropora* and *Pocillopora* and a 10% decrease for *Porites*.

According to the isometric model, reef-scale $CaCO_3$ production per unit area remained relatively constant (~7 kg $CaCO_3$ m^{-2} yr^{-1}; Fig. 4 and Table S1) across the ten-year study period, despite fluctuations in coral cover (Fig. 2). In contrast, the allometric model revealed marked variation in reef-scale $CaCO_3$ production over the same period. $CaCO_3$ production per unit area increased from 9 kg $CaCO_3$ m^{-2} yr^{-1} during pre-disturbance in 2005 to 17 kg $CaCO_3$ m^{-2} yr^{-1} in 2010 and 22 kg $CaCO_3$ m^{-2} yr^{-1} in 2013 during reef recovery (Fig. 4a and Table S1). These peaks co-occurred with the recolonization of juvenile corals (Adjeroud et al., 2018), initiated in 2006 in response to the *Acanthaster* outbreak, but it was interrupted by the cyclone in 2010 (Kayal et al., 2012). After 2013, coral colonies grew steadily, leading to a gradual decline in the production of $CaCO_3$ per unit area. Overall, the isometric model led to a 40% underestimation of the total $CaCO_3$ produced over the ten-year period compared to our allometric model (Fig. 4b).

309 To test how reduced coral recruitment impacts reef-scale $CaCO_3$ production, we
310 simulated coral community composition and size structure across a five-year recovery
311 period under four different scenarios of decline in coral recruitment (0%, 25%, 50%,
312 and 75% declines). Recruitment declines dramatically reduced $CaCO_3$ production, with
313 a 68% reduction in $CaCO_3$ production when recruitment is reduced by 75% (Fig. 5).
314 Even a moderate decline of 25% in recruitment reduced post-disturbance $CaCO_3$
315 production by ~30% over a five-year period.
316

317 ## 4 | DISCUSSION

318 **Our study demonstrates that** three major reef-building corals in Mo'orea
319 (*Acropora hyacinthus*, *Pocillopora verrucosa*, and *Porites lutea*) **show** allometric linear
320 extension and **$CaCO_3$ production** patterns. Using the allometric patterns to quantify
321 reef-scale $CaCO_3$ production from coral size structure time-series in Mo'orea indicates
322 that the conventional isometric approach leads to a 40% underestimation of $CaCO_3$
323 production over a ten-year period. Our results imply that recovering reefs have
324 exceptionally high calcification rates due to the fast growth of juvenile corals. Thus,
325 static metrics of coral community assemblages, particularly percent of live coral cover,

may mask dynamic processes that underpin the functioning of reefs, such as $CaCO_3$ production (Brandl et al., 2019).

Over a 10-year-period in Mo'orea, assumption of isometry resulted in an average underestimation of 3 kg m^{-2} yr^{-1}, which equals approximately half of the bioerosion caused by sea urchins and parrotfishes around Mo'orea per year (i.e., ~6 kg m^{-2} yr^{-1} ; Alvarado et al., 2016; Peyrot-Clausade et al., 2000). Although allometric growth, when expressed as an increase in planar area, has been documented for corals (Dornelas et al., 2017), this pattern most likely arose from the higher probability of partial mortality in larger colonies, and thus lower increases in planar area (Kayal et al., 2015; Madin et al., 2020; Pratchett et al., 2015), rather than inherent differences in growth rate across ontogeny. Our *ex situ* estimates of $CaCO_3$ production were not sensitive to the potential effects of partial mortality for two reasons. First, they are nearly instantaneous measures (Gattuso et al., 1998) on small colonies in which partial mortality is less prevalent. Second, partial mortality is often due to predation or overgrowth, which are easily excluded in controlled *ex situ* experiments. Although alizarin red-S staining was conducted in the field, where partial mortality can be observed, we carefully selected healthy branches that did not show signs of predation

343 or overgrowth. Thus, allometric growth likely results from shifts in the energy allocated
344 to $CaCO_3$ production across the colony size gradient. Indeed, larger colonies may
345 invest substantial energy in reproduction, which might reduce the energy available for
346 calcification (Kayal et al., 2015).

347 Our findings also have important implications for our understanding of system-
348 wide reef accretion rates under climate change. Indeed, reef accretion depends on the
349 net community production of $CaCO_3$ (Perry et al., 2012) and our results suggest that,
350 after a perturbation, small colonies may greatly bolster community-level $CaCO_3$
351 production (see also Gilmour et al., 2013). However, the presence of juvenile corals
352 strongly depends on the reproductive capacity of mature coral colonies (Edmunds,
353 2017; Holbrook et al., 2018; Vercelloni et al., 2019). Severe, large-scale, and repeated
354 disturbances can dramatically erode the supply of coral recruits to large swaths of
355 reefs. For example, coral recruitment on the Australian Great Barrier Reef in 2018
356 declined by 89% in response to the loss of corals during 2016 and 2017 bleaching
357 events (Hughes et al., 2019). Our results indicate that disruption and decline of coral
358 recruitment may lead to a decrease in the production of $CaCO_3$ with a potentially
359 profound impact on reef accretion. In fact, because juvenile corals play a

360 disproportionate role in $CaCO_3$ production, reductions in coral recruitment following
361 disturbances, such as extensive coral bleaching, may undermine the capacity of reef
362 ecosystems to recover and, ultimately, **endanger** the persistence of reefs that protect
363 tropical coasts (Oppenheimer et al., 2019).

364 Area-normalized $CaCO_3$ production showed a nearly inverted profile (Fig. 4a)
365 compared to coral cover, emphasizing the deep divide between metrics of ecosystem
366 function (e.g., growth, $CaCO_3$ production) and their outcomes (e.g., coral cover,
367 **structural complexity**). As a consequence, much of coral reef monitoring is likely to
368 evaluate outcomes of past reef configurations rather than current levels of functioning.
369 To efficiently monitor and protect coral reefs in times of unprecedented anthropogenic
370 and climatic impacts, our results emphasize the need to move beyond ecosystem
371 assessments based solely on static surveys (e.g., coral cover or fish biomass) and
372 consider metrics that quantify reef functioning as a dynamic process (Brandl, Rasher,
373 et al., 2019; Darling et al., 2012; Edmunds & Riegl, 2020; Madin et al., 2016).

374 Overall, we provide a novel perspective on coral reef $CaCO_3$ production that
375 has direct implications for the security of coastal populations throughout the tropics
376 (Arkema et al., 2013; Perry, Alvarez-Filip, et al., 2018). With current projections of

global change, reefs will face disturbances such as coral bleaching at increasing frequencies. After these disturbances, juvenile corals can **buffer the decrease in community $CaCO_3$ production caused by live coral loss through their rapid growth.** However, reductions in coral recruitment, as recorded after large-scale disturbances, will undermine this buffering capacity, ultimately **hampering vertical reef accretion and consequently the protection** of tropical coasts from oceanic waves. **The buffering capacity of small colonies provides only a short term boost (until colonies grow bigger) that may support a faster return to pre-disturbance levels of coral cover and reef structural complexity. Yet, vertical reef accretion happens over a much longer time frame and relies on several other factors such as substrate cementation by coralline algae and sediment input (Perry et al., 2012; Perry, Lange, et al., 2018). Thus, despite the capacity of juvenile corals to temporarily accelerate reef recovery through rapid growth, long-term persistence of coral reefs and their services inevitably hinge on the preservation of coral populations across size classes.**

Acknowledgements: We thank the "*Service d'Observatoire CORAIL*" (SO CORAIL) and the Mo'orea Coral Reef Long Term Ecological Research (LTER) programs.

394 Thanks also to Yann Lacube and Adeline Goyaud for help with alizarin red-S staining,
395 Martin Alessandrini and Hmeniko Tourancheau for help defining linear coral extension
396 rates, technical support from the Université de Perpignan and the Banyuls sur Mer
397 Observatory (Fabien Morat, Guillaume Iwankow, Titouan Morage and David
398 Pecqueur) and Joshua Madin for reviewing our manuscript before submission.
399 **Funding:** This research was supported by the BNP Foundation (Reef Services Project),
400 the French Polynesian government (RisqueRecif Project), the Fondation de France
401 (Acid Reefs project) the Fondation pour la Recherche et Biodiversité and Ministère de
402 la Transition Ecologique et Solidaire (Acid Reefs 2 project). This research is also
403 product of the SCORE-REEF group funded by the Centre de Synthèse et d'Analyse
404 sur la Biodiversité (CESAB) of the Foundation pour la Recherche sur la Biodiversité
405 (FRB) and the Agence Nationale de la Biodiversité (AFB). VP was supported by the
406 Institut Universitaire de France (IUF), JMC was supported by a Make Our Planet Great
407 Again Postdoctoral Grant (mopga-pdf-0000000144). **Author contributions:** J.C and V.P
408 conceived the idea and methods. J.C performed the alizarin red-S staining, and J.C,
409 A.M, B.E and U.C performed the incubation experiments. M.A, H.S.L. and M.K
410 performed the size distribution surveys. J.C. performed the photogrammetry. J.C.

created the growth model and M.K. built the recruitment scenarios model. J.C wrote the first draft of the paper, and all co-authors contributed to revisions and approved the final draft. **Competing interests**: None declared. **Data availability:** Code and data are available on https://github.com/JayCrlt/Allometric_coral_growth.git

REFERENCES

Adjeroud, M., Kayal, M., Iborra-Cantonnet, C., Vercelloni, J., Bosserelle, P., Liao, V., Chancerelle, Y., Claudet, J., & Penin, L. (2018). Recovery of coral assemblages despite acute and recurrent disturbances on a South Central Pacific reef. *Scientific Reports*, *8*(1), 9680. https://doi.org/10.1038/s41598-018-27891-3

Adjeroud, M., Mauguit, Q., & Penin, L. (2015). The size-structure of corals with contrasting life-histories: A multi-scale analysis across environmental conditions. *Marine Environmental Research*, *112*, 131–139. https://doi.org/https://doi.org/10.1016/j.marenvres.2015.10.004

Alvarado, J. J., Cortés, J., Guzman, H., & Reyes-Bonilla, H. (2016). Bioerosion by the sea urchin Diadema mexicanum along Eastern Tropical Pacific coral reefs. *Marine Ecology*, *37*(5), 1088–1102. https://doi.org/https://doi.org/10.1111/maec.12372

Arkema, K. K., Guannel, G., Verutes, G., Wood, S. A., Guerry, A., Ruckelshaus, M., Kareiva, P., Lacayo, M., & Silver, J. M. (2013). Coastal habitats shield people and property from sea-level rise and storms. *Nature Climate Change*, *3*(10), 913–918. https://doi.org/10.1038/nclimate1944

Brandl, S., Rasher, D. B., Côté, I. M., Casey, J. M., Darling, E. S., Lefcheck, J. S., & Duffy, J. E. (2019). Coral reef ecosystem functioning: eight core processes and the role of biodiversity. *Frontiers in Ecology and the Environment*, *17*(8), 445–454. https://doi.org/https://doi.org/10.1002/fee.2088

Brandl, S., Tornabene, L., Goatley, C. H. R., Casey, J. M., Morais, R. A., Côté, I. M., Baldwin, C. C., Parravicini, V., Schiettekatte, N. M. D., & Bellwood, D. R. (2019). Demographic dynamics of the smallest marine vertebrates fuel coral reef ecosystem functioning. *Science*, *364*(6446), 1189 LP – 1192. https://doi.org/10.1126/science.aav3384

Bürkner, P.-C. (2017a). *Advanced Bayesian Multilevel Modeling with the R Package brms*.

Bürkner, P.-C. (2017b). brms: An R Package for Bayesian Multilevel Models Using Stan. *Journal of Statistical Software; Vol 1, Issue 1 (2017)* . https://doi.org/10.18637/jss.v080.i01

Carlot, J., Rovère, A., Casella, E., Harris, D., Grellet-Muñoz, C., Chancerelle, Y., Dormy, E., Hedouin, L., & Parravicini, V. (2020). Community composition predicts photogrammetry-based structural complexity on coral reefs. *Coral Reefs*, *39*(4), 967–975. https://doi.org/10.1007/s00338-020-01916-8

Darling, E. S., Alvarez-Filip, L., Oliver, T. A., McClanahan, T. R., & Côté, I. M. (2012). Evaluating life-history strategies of reef corals from species traits. *Ecology Letters*, *15*(12), 1378–1386. https://doi.org/https://doi.org/10.1111/j.1461-0248.2012.01861.x

Darling, E. S., McClanahan, T. R., Maina, J., Gurney, G. G., Graham, N. A. J., Januchowski-Hartley, F., Cinner, J. E., Mora, C., Hicks, C. C., Maire, E., Puotinen, M., Skirving, W. J., Adjeroud, M., Ahmadia, G., Arthur, R., Bauman, A. G., Beger, M., Berumen, M. L., Bigot, L., … Mouillot, D. (2019). Social–environmental drivers inform strategic management of coral reefs in the Anthropocene. *Nature Ecology & Evolution*, *3*(9), 1341–1350. https://doi.org/10.1038/s41559-019-0953-8

Dickson, A. G., Sabine, C. L., & Christian, J. R. (2007). *Guide to best practices for ocean CO2 measurements.* North Pacific Marine Science Organization.

Dietzel, A., Bode, M., Connolly, S. R., & Hughes, T. P. (2020). Long-term shifts in the colony size structure of coral populations along the Great Barrier Reef. *Proceedings of the Royal Society B: Biological Sciences*, *287*(1936), 20201432. https://doi.org/10.1098/rspb.2020.1432

Dornelas, M., Madin, J. S., Baird, A. H., & Connolly, S. R. (2017). Allometric growth in reef-building corals. *Proceedings of the Royal Society B: Biological Sciences*, *284*(1851), 20170053. https://doi.org/10.1098/rspb.2017.0053

Edmunds, P. J. (2017). Unusually high coral recruitment during the 2016 El Niño in Mo'orea, French Polynesia. *PLOS ONE*, *12*(10), e0185167. https://doi.org/10.1371/journal.pone.0185167

Edmunds, P. J., & Riegl, B. (2020). Urgent need for coral demography in a world where corals are disappearing. *Marine Ecology Progress Series*, *635*, 233–242. https://www.int-res.com/abstracts/meps/v635/p233-242/

Ellison, J. C., Han, P., & Lewis, T. W. (2019). Carbonate beach sand of Abaiang Atoll, Kiribati: geochemistry, biogenic sources, and properties. *Atoll Research Bulletin*, *621*, 1–21.

Gattuso, J.-P., Frankignoulle, M., Bourge, I., Romaine, S., & Buddemeier, R. W. (1998).

Effect of calcium carbonate saturation of seawater on coral calcification. *Global and Planetary Change*, *18*(1), 37–46. https://doi.org/https://doi.org/10.1016/S0921-8181(98)00035-6

Gilmour, J. P., Smith, L. D., Heyward, A. J., Baird, A. H., & Pratchett, M. S. (2013). Recovery of an Isolated Coral Reef System Following Severe Disturbance. *Science*, *340*(6128), 69 LP – 71. https://doi.org/10.1126/science.1232310

Harris, D. L., Rovere, A., Casella, E., Power, H., Canavesio, R., Collin, A., Pomeroy, A., Webster, J. M., & Parravicini, V. (2018). Coral reef structural complexity provides important coastal protection from waves under rising sea levels. *Science Advances*, *4*(2), eaao4350. https://doi.org/10.1126/sciadv.aao4350

Hoegh-Guldberg, O., Mumby, P. J., Hooten, A. J., Steneck, R. S., Greenfield, P., Gomez, E., Harvell, C. D., Sale, P. F., Edwards, A. J., Caldeira, K., Knowlton, N., Eakin, C. M., Iglesias-Prieto, R., Muthiga, N., Bradbury, R. H., Dubi, A., & Hatziolos, M. E. (2007). Coral Reefs Under Rapid Climate Change and Ocean Acidification. *Science*, *318*(5857), 1737 LP – 1742. https://doi.org/10.1126/science.1152509

Holbrook, S. J., Adam, T. C., Edmunds, P. J., Schmitt, R. J., Carpenter, R. C., Brooks, A. J., Lenihan, H. S., & Briggs, C. J. (2018). Recruitment Drives Spatial Variation in Recovery Rates of Resilient Coral Reefs. *Scientific Reports*, *8*(1), 7338. https://doi.org/10.1038/s41598-018-25414-8

Hughes, T. P., Kerry, J. T., Álvarez-Noriega, M., Álvarez-Romero, J. G., Anderson, K. D., Baird, A. H., Babcock, R. C., Beger, M., Bellwood, D. R., Berkelmans, R., Bridge, T. C., Butler, I. R., Byrne, M., Cantin, N. E., Comeau, S., Connolly, S. R., Cumming, G. S., Dalton, S. J., Diaz-Pulido, G., … Wilson, S. K. (2017). Global warming and recurrent mass bleaching of corals. *Nature*, *543*(7645), 373–377. https://doi.org/10.1038/nature21707

Hughes, T. P., Kerry, J. T., Baird, A. H., Connolly, S. R., Chase, T. J., Dietzel, A., Hill, T., Hoey, A. S., Hoogenboom, M. O., Jacobson, M., Kerswell, A., Madin, J. S., Mieog, A., Paley, A. S., Pratchett, M. S., Torda, G., & Woods, R. M. (2019). Global warming impairs stock–recruitment dynamics of corals. *Nature*, *568*(7752), 387–390. https://doi.org/10.1038/s41586-019-1081-y

Hughes, T. P., & Tanner, J. E. (2000). RECRUITMENT FAILURE, LIFE HISTORIES, AND LONG-TERM DECLINE OF CARIBBEAN CORALS. *Ecology*, *81*(8), 2250–2263. https://doi.org/https://doi.org/10.1890/0012-9658(2000)081[2250:RFLHAL]2.0.CO;2

Kayal, M., Lenihan, H. S., Brooks, A. J., Holbrook, S. J., Schmitt, R. J., & Kendall, B. E. (2018). Predicting coral community recovery using multi-species population dynamics models. *Ecology Letters*, *21*(12), 1790–1799.

https://doi.org/https://doi.org/10.1111/ele.13153

Kayal, M., Vercelloni, J., Lison de Loma, T., Bosserelle, P., Chancerelle, Y., Geoffroy, S., Stievenart, C., Michonneau, F., Penin, L., Planes, S., & Adjeroud, M. (2012). Predator Crown-of-Thorns Starfish (Acanthaster planci) Outbreak, Mass Mortality of Corals, and Cascading Effects on Reef Fish and Benthic Communities. *PLOS ONE*, *7*(10), e47363. https://doi.org/10.1371/journal.pone.0047363

Kayal, M., Vercelloni, J., Wand, M. P., & Adjeroud, M. (2015). Searching for the best bet in life-strategy: A quantitative approach to individual performance and population dynamics in reef-building corals. *Ecological Complexity*, *23*, 73–84. https://doi.org/https://doi.org/10.1016/j.ecocom.2015.07.003

Kolb, R. W. (2018). National Ambient Air Quality Standards (NAAQS). In *The SAGE Encyclopedia of Business Ethics and Society*. SAGE Publications, Inc. https://doi.org/10.4135/9781483381503.n817

LLC, Agisoft (2016). Agisoft PhotoScan User Manual : Professional Edition, Version 1.2. In *User Manuals* (p. 97). http://www.agisoft.com/downloads/user-manuals/

Madin, J. S., Anderson, K. D., Andreasen, M. H., Bridge, T. C. L., Cairns, S. D., Connolly, S. R., Darling, E. S., Diaz, M., Falster, D. S., Franklin, E. C., Gates, R. D., Harmer, A. M. T., Hoogenboom, M. O., Huang, D., Keith, S. A., Kosnik, M. A., Kuo, C.-Y., Lough, J. M., Lovelock, C. E., … Baird, A. H. (2016). The Coral Trait Database, a curated database of trait information for coral species from the global oceans. *Scientific Data*, *3*(1), 160017. https://doi.org/10.1038/sdata.2016.17

Madin, J. S., Baird, A. H., Baskett, M. L., Connolly, S. R., & Dornelas, M. A. (2020). Partitioning colony size variation into growth and partial mortality. *Biology Letters*, *16*(1), 20190727. https://doi.org/10.1098/rsbl.2019.0727

Morais, R. A., & Bellwood, D. R. (2019). Pelagic Subsidies Underpin Fish Productivity on a Degraded Coral Reef. *Current Biology*, *29*(9), 1521-1527.e6. https://doi.org/https://doi.org/10.1016/j.cub.2019.03.044

Nunn, P., Kohler, A., & Kumar, R. (2017). Identifying and assessing evidence for recent shoreline change attributable to uncommonly rapid sea-level rise in Pohnpei, Federated States of Micronesia, Northwest Pacific Ocean. *Journal of Coastal Conservation*, *21*(6), 719–730. https://doi.org/10.1007/s11852-017-0531-7

Oppenheimer, M., Glavovic, B., Hinkel, J., van de Wal, R., Magnan, A. K., Abd-Elgawad, A., Cai, R., Cifuentes-Jara, M., DeConto, R. M., Ghosh, T., Hay, J., Isla, F., Marzeion, B., Meyssignac, B., & Sebesvari, Z. (2019). Sea Level Rise and Implications for Low Lying Islands, Coasts and Communities. *IPCC Special Report on the Ocean and Cryosphere in a Changing Climate*, *355*(6321), 126–129.

Perry, C. T., Alvarez-Filip, L., Graham, N. A. J., Mumby, P. J., Wilson, S. K., Kench, P. S., Manzello, D. P., Morgan, K. M., Slangen, A. B. A., Thomson, D. P., Januchowski-Hartley, F., Smithers, S. G., Steneck, R. S., Carlton, R., Edinger, E. N., Enochs, I. C., Estrada-Saldívar, N., Haywood, M. D. E., Kolodziej, G., … Macdonald, C. (2018). Loss of coral reef growth capacity to track future increases in sea level. *Nature*, *558*(7710), 396–400. https://doi.org/10.1038/s41586-018-0194-z

Perry, C. T., Edinger, E. N., Kench, P. S., Murphy, G. N., Smithers, S. G., Steneck, R. S., & Mumby, P. J. (2012). Estimating rates of biologically driven coral reef framework production and erosion: a new census-based carbonate budget methodology and applications to the reefs of Bonaire. *Coral Reefs*, *31*(3), 853–868. https://doi.org/10.1007/s00338-012-0901-4

Perry, C. T., Lange, I., & Januchowski-Hartley, F. A. (2018). *ReefBudget Indo-Pacific: online resource and methodology, http://geography.exeter.ac.uk/reefbudget/.*

Peyrot-Clausade, M., Chabanet, P., Conand, C., Fontaine, M. F., Letourneur, Y., & Harmelin-Vivien, M. (2000). Sea urchin and fish bioerosion on La Réunion and Moorea reefs. *Bulletin of Marine Science*, *66*(2), 477–485.

Pinheiro, J., Bates, D., DebRoy, S., Sarkar, D., & Team, R. C. (2013). nlme: Linear and nonlinear mixed effects models. *R Package Version*, *3*(1), 111.

Pratchett, M. S., Anderson, K. D., Hoogenboom, M. O., Widman, E., Baird, A. H., Pandolfi, J. M., Edmunds, P. J., & Lough, J. M. (2015). Spatial, temporal and taxonomic variation in coral growth-implications for the structure and function of coral reef ecosystems. In *Oceanography and Marine Biology: An Annual Review* (Vol. 53, pp. 215–295). CRC Press. https://doi.org/10.1201/b18733

R Core Team. (2019). *R: A Language and Environment for Statistical Computing*.

Schneider, C. A., Rasband, W. S., & Eliceiri, K. W. (2012). NIH Image to ImageJ: 25 years of image analysis. *Nature Methods*, *9*(7), 671–675. https://doi.org/10.1038/nmeth.2089

Smith, L. W., Barshis, D., & Birkeland, C. (2007). Phenotypic plasticity for skeletal growth, density and calcification of Porites lobata in response to habitat type. *Coral Reefs*, *26*(3), 559–567. https://doi.org/10.1007/s00338-007-0216-z

Smith, S. V, & Key, G. S. (1975). Carbon dioxide and metabolism in marine environments. *Limnology and Oceanography*, *20*(3), 493–495.

Tebaldi, C., Strauss, B. H., & Zervas, C. E. (2012). Modelling sea level rise impacts on storm surges along US coasts. *Environmental Research Letters*, *7*(1), 14032. https://doi.org/10.1088/1748-9326/7/1/014032

van Hooidonk, R., Maynard, J., Tamelander, J., Gove, J., Ahmadia, G., Raymundo, L., Williams, G., Heron, S. F., & Planes, S. (2016). Local-scale projections of coral reef

586 futures and implications of the Paris Agreement. *Scientific Reports*, *6*(1), 39666.
587 https://doi.org/10.1038/srep39666
588 Vercelloni, J., Kayal, M., Chancerelle, Y., & Planes, S. (2019). Exposure, vulnerability, and
589 resiliency of French Polynesian coral reefs to environmental disturbances. *Scientific*
590 *Reports*, *9*(1), 1027. https://doi.org/10.1038/s41598-018-38228-5
591 Woodroffe, C. D., & Webster, J. M. (2014). Coral reefs and sea-level change. *Marine*
592 *Geology*, *352*, 248–267. https://doi.org/https://doi.org/10.1016/j.margeo.2013.12.006
593

Figure 1

Conceptual diagram describing isometric versus allometric $CaCO_3$ production curves. Size dependent metabolic production characterized by (a) a linearly increasing model with coral surface area (isometric metabolic curve in orange; equation $y = \alpha x + 0$), and (b) a logarithmic asymptote (allometric metabolic curve in blue; equation $y = \alpha x^{\beta} + 0$). The dashed line indicates the size at which the two curves cross (i.e. this threshold point depends on both the intercepts and the allometric scaling slopes). Compared to the allometric model, the isometric model may underestimate $CaCO_3$ production below this threshold and overestimate $CaCO_3$ production at lager coral sizes.

Figure 2

Average live coral cover in Mo'orea, French Polynesia, from 2005 to 2016. Perturbations included a predatory sea star (*Acanthaster* cf. *solaris*) outbreak from 2006 to 2009 and a cyclone in 2010. Photographs illustrate the reefscape in (a) 2006, (b) 2010 and (c) 2015.

Figure 3

$CaCO_3$ production rates of the three reef-building coral species. On the left. changes in linear extension for the coral species *A. hyacinthus, P. verrucosa* and *P. lutea* as a function of colony size. On the right, changes in $CaCO_3$ production rates as a function of colony size. $CaCO_3$ production was estimated using two growth measurement methods (*in situ* alizarin red-S staining and *ex situ* metabolic incubations).

Figure 4

Coral community $CaCO_3$ production estimates of a $10m^2$ portion of reef substrate in Mo'orea from 2005 to 2016 according to the isometric versus allometric coral **$CaCO_3$ production** models. (a) $CaCO_3$ production rate (kg m^{-2} yr^{-1}), (b) cumulative $CaCO_3$ production (kg yr^{-1}). Estimates are bounded by a 95% confidence interval. Coral symbols on top indicate changes in average coral colony size, and numbers indicate coral colony density per $10m^2$ of reef surface area.

Figure 5

Normalized $CaCO_3$ production trajectories according to four scenarios of coral recruitment over five years during reef recovery. A multi-species, open-population integral projection model was used to predict the recovery dynamics of an assemblage of three coral genera (*Acropora, Pocillopora* and *Porites*) based on coral demographic performance (in recruitment, growth, and survival) measured in Mo'orea. The four scenarios predicted different rates of coral recruitment reduction as compared to current levels (0%, 25%, 50% and 75% reductions). $CaCO_3$ production rates were estimated from model predictions of coral abundance, composition and size distribution (Figure S5, combined with the allometric $CaCO_3$ production functions estimated in Mo'orea (Fig. 1). $CaCO_3$ production rates were normalized relative to the highest value (scenario 0% reduction at year 5; green curve).

Figure S1

Map of study sites for the *in situ* alizarin red-S staining. Alizarin red-S staining was conducted on the reef slopes around Mo'orea, French Polynesia, and included 175 colonies **(numbered from 1 to 175 under the gray labels)**. The grey labels indicate the sampling sites. The corals used in the *ex-situ* incubations were collected at Vaipahu, on the north shore of the island.

644

645 **Figure S2**

646 Alizarin red-S staining example. The photographs illustrate a 0.7 mm thick slice from
647 one of the pocilloporid colonies 131 days after staining. (a) Introspected image
648 observed under microscope, and (b) the same slice observed under a fluorescent
649 microscope. (c) A superposition of the two images to define the maximum linear
650 extension of the coral. For this coral fragment, the linear extension was 0.57 cm over
651 131 days, which corresponds to a $CaCO_3$ production rate of 3.1 kg m^{-2} yr^{-1}.

652

653 **Figure S3**

654 **Photogrammetry-based size-area relationships. For each of the three coral species,**
655 **we fitted a power-law regression for the mean diameter (i.e., the mean of the length,**
656 **width and height of each colony) and the live surface area of the coral colonies. We**
657 **also estimated an average trendline across the three coral species (dashed points)**
658 **(R^2=0.97). Coral symbols indicate the growth morphologies of the three coral species.**

659

660 **Figure S4**

661 Compilation of the alizarin red-S and the incubation datasets. The Bayesian allometric
662 $CaCO_3$ model was first characterized for the three coral genera (*Acropora,*
663 *Pocillopora* and *Porites*) with only the alizarin red-S dataset (n=130 top plots). We then
664 merged both alizarin red-S and incubation datasets for defining a more complete
665 allometric $CaCO_3$ production model (n=200, bottom plot). The power-law equations
666 from each species and each dataset were written on the top of each plot. For each of
667 the three species, no significant difference in calcification estimates were found
668 between the alizarin red-S only and both the alizarin red-S and incubation combined
669 datasets (two-tailed t-test; p = 0.93, 0.61 and 0.17 for respectively *Acropora*
670 *hyacinthus, Pocillopora verrucosa* and *Porites lutea*).

671

672 **Figure S5**

673 Robustness of the coral community size distributions data. To test whether our island-
674 scale estimations of coral size-distributions matched the data from locally performed
675 surveys at specific sites around Mo'orea (see Methods section Coral community size
676 distributions), we compared our predictions to the coral size-distribution dataset

observed in Kayal et al. (2015) from the year 2009 and for the genus Pocillopora. Thus, on the left plot, we represented the modeled size-distribution dataset while we described on the right plot, the current observed size-distribution dataset. For both datasets, we observed a peak of several individuals between 0 and 4 cm of diameter. Despite a slight increase for small colonies in the dataset modeled, both patterns are similar, and we found no significant difference between both size-distribution datasets (two-tailed t-test; $p = 0.08$).

Figure S6

Recruitment loss model. Coral community trajectories predicted under four recruitment scenarios over the course of five years (2010-2015). The population dynamics of the three coral taxa are expressed in terms of changes in coral abundance (y-axis) across colony sizes (x-axis) with time (years) and scenarios (0%, 25%, 50% and 75% reductions in recruitment rates). The predicted coral abundances, compositions, and size structures were used to estimate community calcification under the four scenarios (see Fig. 4).

Table S1

Compilation of all estimated variables over the course of ten years. The first three variables correspond with demographic performance within a $10m^2$ transect (number of individuals, average coral diameter, and live coral surface area). The next six variables correspond with estimates of $CaCO_3$ production ($CaCO_3$ production, area-normalized $CaCO_3$ production, and cumulative $CaCO_3$ production for both isometric and allometric $CaCO_3$ production models)

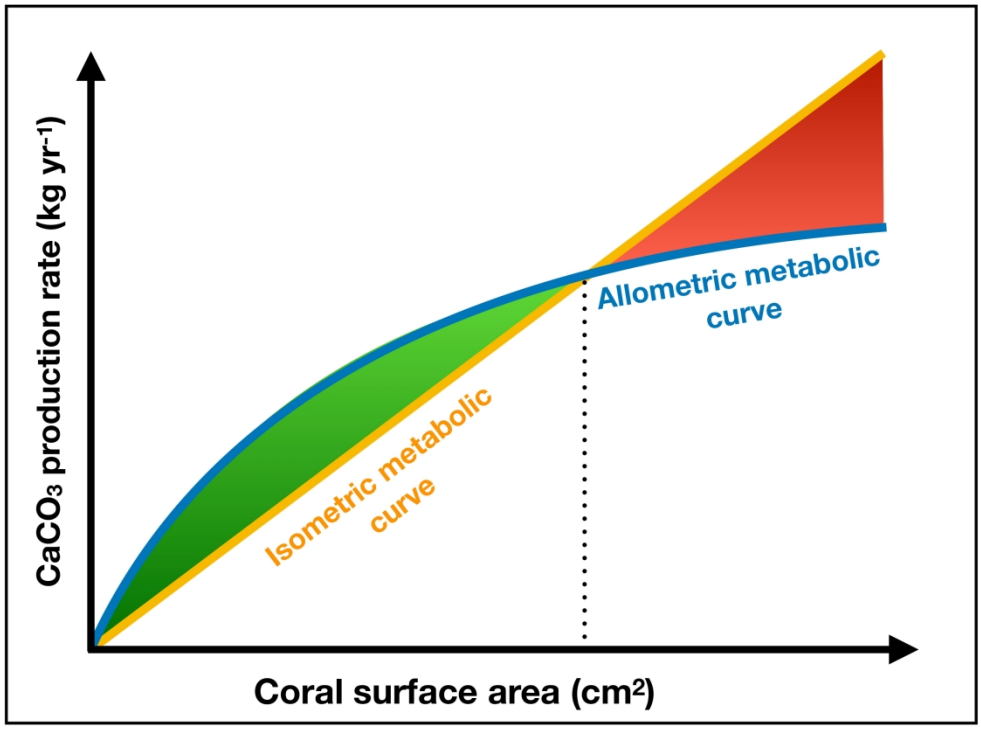

Figure 1: Conceptual diagram describing isometric versus allometric CaCO3 production curves. Size dependent metabolic production characterized by (a) a linearly increasing model with coral surface area (isometric metabolic curve in orange; equation $y = \alpha x + 0$), and (b) a logarithmic asymptote (allometric metabolic curve in blue; equation $y = \alpha x \beta + 0$). The dashed line indicates the size at which the two curves cross (i.e. this threshold point depends on both the intercepts and the allometric scaling slopes). Compared to the allometric model, the isometric model may underestimate CaCO3 production below this threshold and overestimate CaCO3 production at lager coral sizes.

242x181mm (600 x 600 DPI)

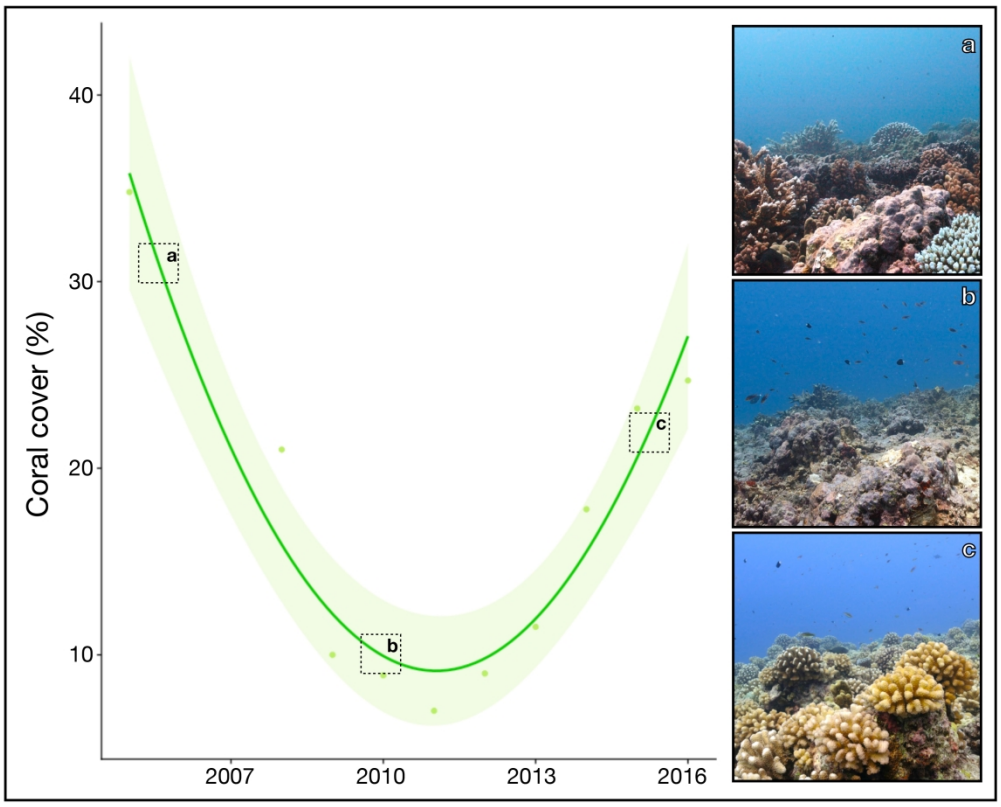

Figure 2: Average live coral cover in Mo'orea, French Polynesia, from 2005 to 2016. Perturbations included a predatory sea star (Acanthaster cf. solaris) outbreak from 2006 to 2009 and a cyclone in 2010. Photographs illustrate the reefscape in (a) 2006, (b) 2010 and (c) 2015.

285x228mm (600 x 600 DPI)

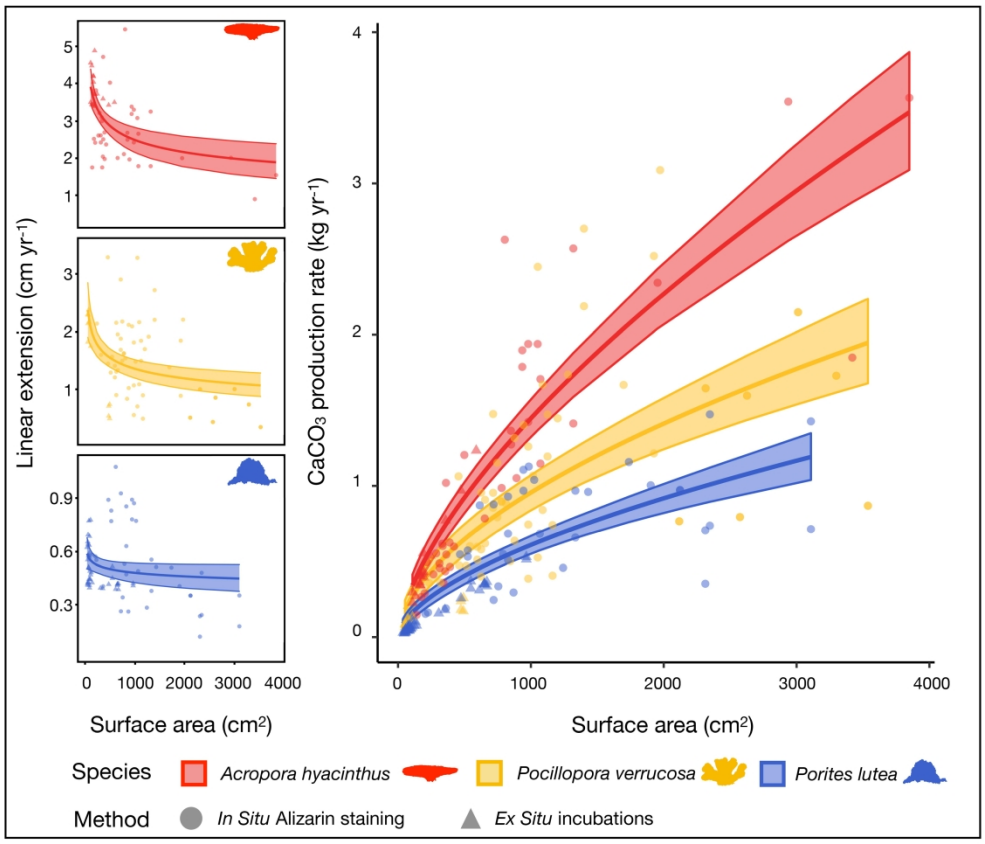

Figure 3: CaCO3 production rates of the three reef-building coral species. On the left. changes in linear extension for the coral species A. hyacinthus, P. verrucosa and P. lutea as a function of colony size. On the right, changes in CaCO3 production rates as a function of colony size. CaCO3 production was estimated using two growth measurement methods (in situ alizarin red-S staining and ex situ metabolic incubations).

246x209mm (600 x 600 DPI)

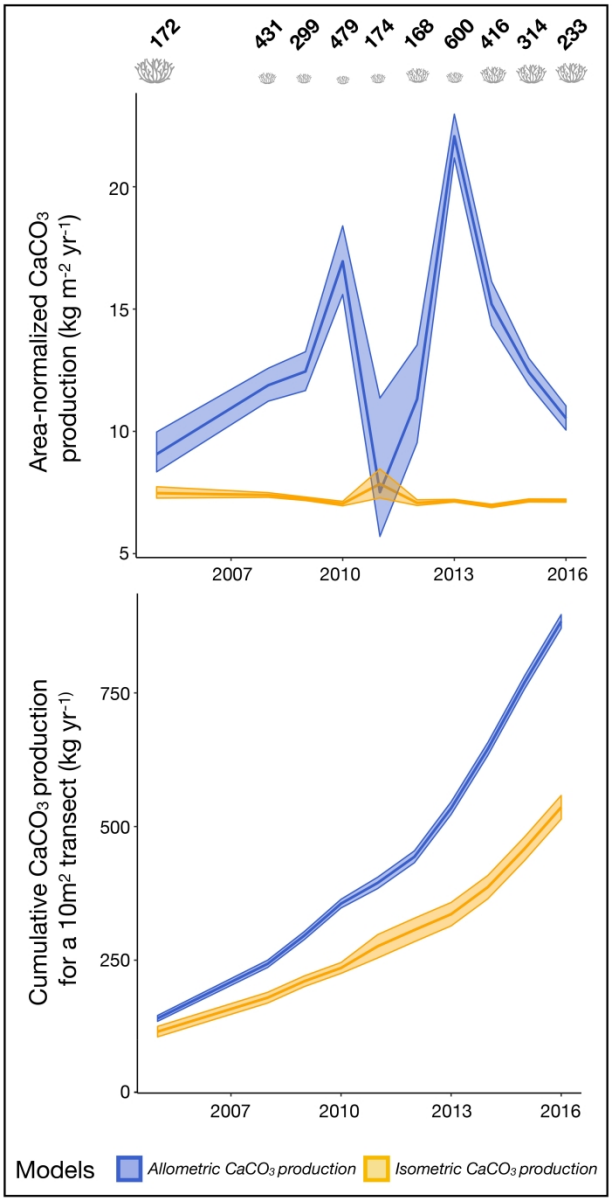

Figure 4: Coral community CaCO3 production estimates of a 10m2 portion of reef substrate in Mo'orea from 2005 to 2016 according to the isometric versus allometric coral growth models. (a) CaCO3 production rate (kg m-2 yr-1), (b) cumulative CaCO3 production (kg yr-1). Estimates are bounded by a 95% confidence interval. Coral symbols on top indicate changes in average coral colony size, and numbers indicate coral colony density per 10m2 of reef surface area.

213x417mm (600 x 600 DPI)

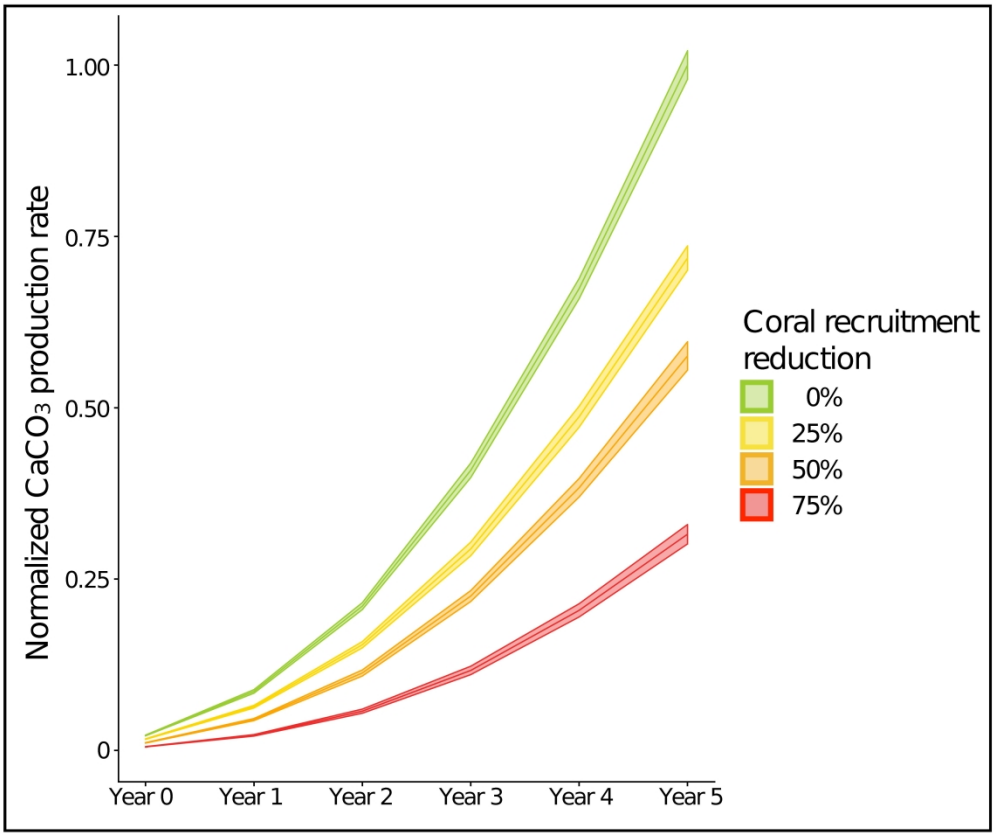

Figure 5: Normalized CaCO3 production trajectories according to four scenarios of coral recruitment over five years during reef recovery. A multi-species, open-population integral projection model was used to predict the recovery dynamics of an assemblage of three coral genera (Acropora, Pocillopora and Porites) based on coral demographic performance (in recruitment, growth, and survival) measured in Mo'orea. The four scenarios predicted different rates of coral recruitment reduction as compared to current levels (0%, 25%, 50% and 75% reductions). CaCO3 production rates were estimated from model predictions of coral abundance, composition and size distribution (Figure S5, combined with the allometric CaCO3 production functions estimated in Mo'orea (Fig. 1). CaCO3 production rates were normalized relative to the highest value (scenario 0% reduction at year 5; green curve).

251x209mm (600 x 600 DPI)